Surface Enhanced Raman Scattering, in Situ Spectro-Electrochemical, and Electrochemical Impedance Spectroscopic Investigations of 2-Amino-5-mercapto-1,3,4-thiadiazole Monolayers at...

ARTICLE *in* THE JOURNAL OF PHYSICAL CHEMISTRY C · MAY 2007

Impact Factor: 4.77 · DOI: 10.1021/jp070439e

6 AUTHORS, INCLUDING:

Haifeng Yang
Shanghai Normal University
64 PUBLICATIONS **882** CITATIONS

SEE PROFILE

Surface Enhanced Raman Scattering, in Situ Spectro-Electrochemical, and Electrochemical Impedance Spectroscopic Investigations of 2-Amino-5-mercapto-1,3,4-thiadiazole Monolayers at a Silver Electrode

Haifeng Yang,* Xiaojing Sun, Jun Zhu, Jiahua Ji, Xiaoling Ma, and Zongrang Zhang

Department of Chemistry, Shanghai Normal University, 100 Guilin Road, Shanghai 200234, People's Republic of China

Received: January 18, 2007; In Final Form: March 6, 2007

At a silver surface, surface-enhanced Raman scattering (SERS) technique along with the self-assembled monolayers (SAMs) method was performed to observe the adsorption behavior of AMT as a protective reagent for metals from corrosion. For 20 h of self-assembling, the time-dependent SERS spectra show that a stable AMT monolayers could form and the ultimate structure of AMT monolayers anchoring at the surface is in tilted mode via both sulfur atoms of thiol and thiadiazole ring with the nitrogen atom of amino. In situ SERS spectral electrochemical experiments indicate that the AMT monolayers experience an dynamic adsorption from a tilted fashion to a more horizontal mode for thiadiazole ring with the potential applied toward more negative voltage. Anticorrosive effect of the AMT monlayers has been ascertained by electrochemical impedance spectroscopy, which is in agreement with theoretic evaluation of the R(Q(R(QR))) mode.

1. Introduction

2-Amino-5-mercapto-1,3,4-thiadiazole (AMT) has been proposed as a newly corrosion inhibitor in the conservation of copper−tin bronzes.[1−4] Its general chemical formula is $C_2H_3N_3S_2$, which is also found under the chemical name of 5-amino-1,3,4-thiadiazole-2-thiol. It is regarded as a planar, pentaheterocyclic compound which is usually white-yellowish powdered crystalline solid at normal temperature.

The complexing behavior of AMT with metal ions was first studied by Gajendragad in 1975.[5,6] His research describes the interaction of AMT with several metal ions, and its ligands are capable of existing in four tautomeric forms with different types of metal ions. The four tautomeric forms are presented in Figure 1.[5,6] Their stability has been proved as follows: I > II > III > IV.[7,8] Ganorkar in 1988 investigated the structural aspects of copper complexes with the AMT ligand by the infrared spectral analysis.[1] AMT can form insoluble complexes with copper ions and has been believed to form a thin polymeric layer over the metal surface. Prado proved that AMT anchored onto silica gel surface by homogeneous and heterogeneous routes.[9] It was characterized by infrared and Raman spectroscopic investigations, superficial area, and elemental analysis as well as ^{13}C and ^{29}Si NMR.

Surface-enhanced Raman scattering (SERS) spectroscopy is a very powerful analytical technique to investigate the interactions of adsorbates with metallic surface,[10−17] because of its high sensitivity and molecular selectivity.[18−23] Although AMT reagent as corrosion inhibitor has been reported for several years, few works are documented on the mechanism of the interactions between the species and metals studied by molecular spectroscopy, especially SERS. In this paper, silver served as an enhanced substrate, adsorption behavior of AMT self-assembled monolayers (SAMs) was observed by potential-dependent in situ SERS spectroscopy. SAMs technique is regarded as a reasonable method to controllably construct an orderly uniform layers that can not only improve the efficiency of anticorrosion but also provide a simple interfacial model for surface analysis.[24−28]

Electrochemical impedance spectroscopy (EIS) as a tool for corrosion study has been extensively used in corrosion inhibitor evaluation. The power of EIS in providing information on the corrosion and protection mechanisms, especially for an adsorbed film was approved.[29−32] Therefore, EIS experiments were performed to clarify the anticorrosive effect of AMT monolayers at the silver surface in aqueous solutions with Cl^-, Br^-, and ClO_4^- anions.

2. Experimental Section

Chemicals. 2-Amino-5-mercapto-1,3,4-thiadiazole (AMT) (98%) was purchased from Sigma-Aldrich Co. and used without further purification. KCl, KBr, $NaClO_4$, and ethanol were of analytical grade. All solutions were prepared from Milli-Q water.

Electrodes. A conventional three-electrode electrochemical cell was used. The working electrode was made from a polycrystalline silver (99.99+%) rod embedded in a Teflon sheath, with a geometric surface area of ca. 0.025 cm^2. A large Pt flake served as the counter electrode. All of the potentials were reported with respect to a saturated calomel electrode (SCE).

The Ag electrode was sequentially polished with emery paper, 1.0, 0.3, and 0.05 μm alumina/water slurries until a shiny, mirror-like finish was obtained. Then the electrode was rinsed successively with copious amounts of Milli-Q water, pure ethanol and treated in an ultrasonic bath to remove any excess of alumina and any carbon oxide produced during the process of polishing.

Activation Procedures. The "activation procedure" is the process to obtain a necessary roughness, which allows the electrode surface to support the SERS effect. The oxidation−reduction cycle (ORC) treatment was used.[33]At first, the clean

* Corresponding author. Tel./fax: +86-21-6432-1648 E-mail: haifengyang@yahoo.com.

10.1021/jp070439e CCC: $37.00
Published on Web 05/16/2007

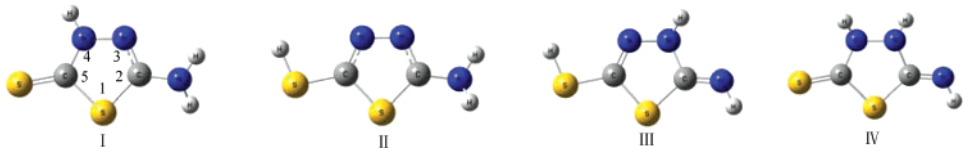

Figure 1. Four tautomeric forms of AMT.

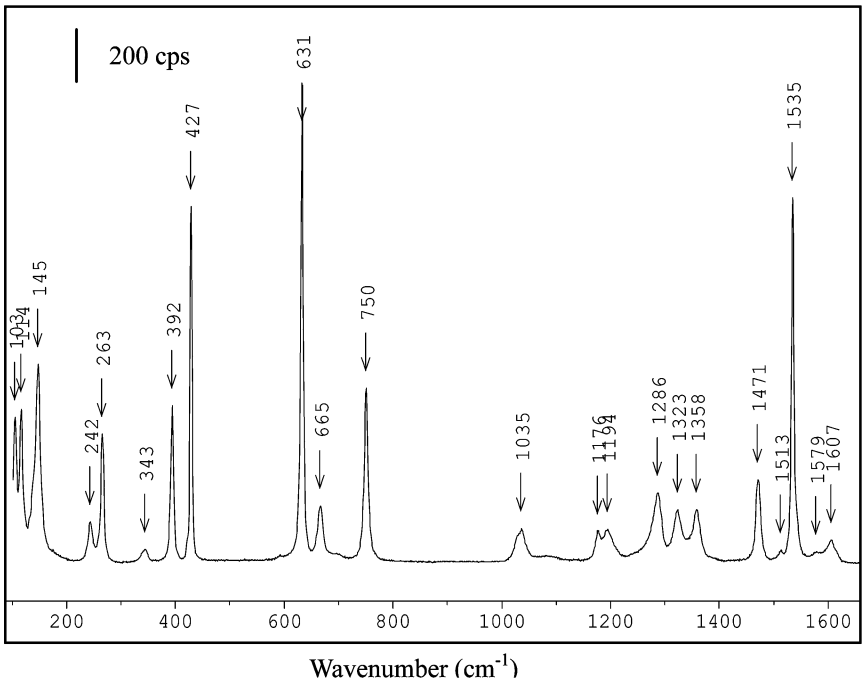

Figure 2. Normal Raman spectra of powder AMT.

Ag electrode was installed to a separate electrochemical cell with 0.1 mol L^{-1} KCl solution for roughening. The electrode was first polarized at −0.25 V for 20 s, and then scanned up to +0.17 V, where the potential was held for 15 s. Then the potential was stepped back to −0.25 V to complete a thorough reduction of the electrode surface. The roughened silver electrode was washed thoroughly with Milli-Q water. After the process all above, the metallic thin film used as SERS substrate was created. All of the ORC procedures were carried out without the presence of the sample in the solution.

In Situ SERS Measurements and Electrochemical Study. *Self-Assembled Monolayers.* The activated electrode was exposed to an aqueous solution containing 0.75×10^{-3} mol L^{-1} AMT. After immersion for 20 h, the electrode was taken out of the solution, washed extensively and dried by flowing nitrogen gas, and a single-layer molecular film was received.

In Situ SERS Measurement. For the in situ SERS experiments, a potential of −0.1 V was applied to the working electrode at least for 5 min. Then the in situ SERS spectra were obtained at different applied potentials from −0.1 to −1.1 V in 0.1 mol L^{-1} KCl, KBr or $NaClO_4$ aqueous solutions.

Electrochemical Study. Electrochemical impedance spectroscopy (EIS) of the silver electrodes was carried out, in the presence and absence of AMT monolayers in different aqueous medium to evaluate the ability of protection from silver corrosion.

Instrumentation. SERS spectra were recorded with a confocal microprobe Raman system (SuperLabRam II from Dilor, France). It comprises an integral Olympus BX40 microscope with a 50 × long working-length objective (8 mm), which was not necessary to be immersed in the solution. A notch filter was used to cut the exciting line and a holographic grating (1800 g/mm) provides a spectral resolution of 4 cm^{-1}. A liquid-nitrogen cooled 1024 × 800 pixels CCD was the detector. The exciting wavelength was 632.8 nm from a He−Ne laser with a power of ca. 5 mW and a spot of the diameter ca. 3 μm on the silver surface. The slit and pinhole were respectively set at 100 and 1000 μm, respectively, in a confocal configuration to increase the spatial resolution. The acquisition time was 15 s, and for each spectrum, there were three accumulations. All the SERS experiments were performed at the ambient condition.

A Princeton Applied Research Potentiostat/Galvanostat Model 283 and a Frequency Response Detector Model 1025 with software M398 were used for EIS measurements. The measurements were carried out at open circuit potential with amplitude of 5 mV in the frequency range from about 1 mHz to 100 kHz. However, the ORC treatment was conducted by CHI 750 electrochemistry work station.

Theoretical Methods. Full geometry optimization and computation of vibration modes for AMT were performed by BLYP/6-311G or PM3 semi-experience methods in Gaussian 98 software.

3. Results and Discussion

Normal Raman Spectra of AMT. To help interpret the SERS spectra of AMT on silver, normal Raman spectrum of AMT in pure powder state is shown in Figure 2. The vibrational assignments are summarized in Table 1 with the calculated results of the four AMT tautomeric forms. It should be pointed out that the full geometry optimization and computation of vibrational modes of AMT isomers I and II were performed by BLYP/6-311G method, and the isomers III and IV were calculated by BLYP/6-311G with polarization and diffuse functions.

TABLE 1: Normal Raman, SERS Spectra, and BLYP/6-311G Calculated Frequencies of AMT with Their Assignments[a]

		calculated			calculated		
solid	SERS	I	II	approximate assignment	III	IV	approximate assignment
114 (m)		113	124	NH_2 wag.	116		S−H wag
145(s)			182	S−H wag.		219	N^4−H wag., N^3−H wag.
241 (w)		233	207	SH rock, NH_2 rock	240		H−S═C^5 wag
263 (m)			256	NH_2 twis., S−H wag.		251	C^5═S rock, NH rock
343 (w)	349 (w)	353	341	N−H wag., ring oop bend			
392 (m)	398 (w)	372	390	NH_2 rock, ring ip bend	395	407	NH rock, ring ip bend
427(s)	430 (w)	415		S═C−S s. str., ring ip bend	416	416	N^4−Hrock, N^3−H rock. ring ip bend
	518 (w)	516		NH_2 twis., H−N^4−C twis.		535	C^2−N^3−H twis., S−C^5═N^4 twis.
	557 (w)	539	533	C−S−C as. str., N−H rock, ring ip bend	565		NH wag. ring oop bend, SH rock
631(s)	630 (w)	599		ring C^2−S str., NH_2 rock		630	N^3−H rock, ring oop bend
665 (m)	658 (w)				634		C^2−S^1 str., HN^3C^2N sciss., NH rock
	684 (w)	667		N^4−H wag.	696		NH wag.
750(s)	776 (w)	733	728	ring ip bend, C^2−N str., S−C−S as. str.	747	751	ring ip bend, NH wag
	851 (w)		871	S−H rock, NH_2 rock		1038	NH rock, N^3−H wag.,
1035 (w)	1043 (sh)			NH_2 rock, N^4−H rock[b]	1040		NH rock, C5−S−H rock
	1102 (s)			NH_2 rock[b]		1123	NH rock, N^3H rock, HN^4C^5 sciss.
1176 (w)	1131 (s)	1180	1124	NH_2 rock, C═NN as. str.	1061		NH rock, $C^5N^4N^3$ rock, SH rock
1194 (w)	1201 (m)			N^3−C^4 str.[b]	1164		N^4−N^3 str, N^3−H rock
	1223 (m)			N−H rock[b]		1247	NH, N^4−H rock, ring ip bend
1286 (m)		1287		C^5−N^4 str., N^4−H rock, NH_2 rock	1256		N^3−C^2−N rock, NH rock
1323 (w)			1303	NH_2 rock, N−C−S as. str.		1331	N^4−H rock, N^3−H rock,$C^5N^4N^3$str.
1358 (w)	1358 (s)	1354		ring ip bend, N−C^2 str., N−H rock			
1471 (m)	1390 (s)		1469	ring C^5−N^4 str.		1487	N^4−H rock., N^3−H rock
1513 (w)	1507 (m)	1493		N^4−H rock			
1535 (s)			1574	N−C═N as. str., N−H rock	1562		C^5−N^4 str., N^3−H rock
1579 (w)		1625		N−C═N as. str., NH_2 sciss.	1662		C^2−N str., NH rock
1606 (w)		1687	1683	NH_2 sciss.		1692	C^2═N str., N^3−H twis

[a] w, weak; m, medium; s, strong; sh, shoulder; str., stretch; sciss., scissor; twis., twist; ip, in-plane; oop, out-of-plane; as, asymmetry. Wavenumber are given in cm^{-1}. [b] From PM3 method.

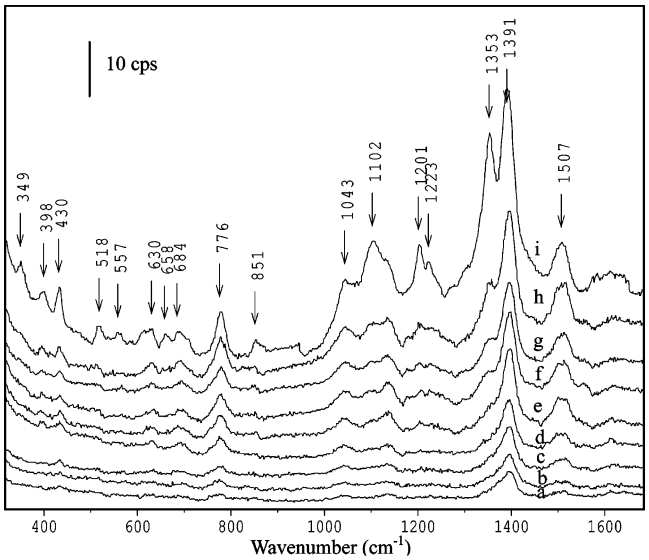

Figure 3. SERS spectra of the formation of SAMs at the silver surface in 0.75×10^{-3} mol L^{-1} AMT aqueous solution a−h in the first 2 h and (i) after 20 h.

In Situ SERS Observation for the Formation of Self-Assembled Monolayers. In order to form monolayers on silver surface, the 0.75×10^{-3} mol L^{-1} AMT solution was introduced into electrochemical cell. The procedure of molecules assembling on the silver surface was recorded by in situ SERS spectra (Figure 3) from the beginning of injection of AMT aqueous solution. As time went by, the peaks were gradually visible. The peaks observed in SERS spectra are much fewer than normal Raman spectra of AMT solid, which should be attributed to the adsorption fashion and the surface selection rules for SERS.[34,35] The assignment to the SERS bands is also listed in Table 1.

It is obvious that at the beginning of immersing the Ag electrode into the AMT aqueous solution, the recorded SERS spectra (Figure 3a−h) are quite different from the SERS spectrum obtained after 20 h. The most differences in the frequency ranging from 1000 to 1600 cm^{-1} see in Figure 3. The bands in primarily obtained SERS spectra for the formation of AMT monolayers appear at 776, 1043, 1131, and 1507 cm^{-1}, also the significantly strong band at 1391 cm^{-1}. The peak at 1043 cm^{-1} belongs to the NH_2 and N^4−H rocking. The mixture of the NH_2 rocking and the C═N−N asymmetric stretching is found near 1131 cm^{-1}. The SERS band at 1391 cm^{-1} is due to the ring C^5−N^4 stretching. A weak scattering occurs around 1507 cm^{-1} arising from the N^4−H rocking. It indicates that the thiadiazole ring approaches toward the silver surface via flat mode at earlier period of the self-assembling.

After 20 h, the relatively stable spectra were obtained and several distinct SERS bands were presented on comparing with the spectra recorded at the start of self-assembly period. From Figure 3i, the most prominent SERS peaks happen at 1201, 1353, and 1391 cm^{-1} due to the ring stretching and in-plane deformation of the AMT. The bands around 349, 398, and 518 cm^{-1} are assigned to the co-contribution of N−H wagging and ring out-of-plane bending, the mixture vibrations of NH_2 rocking and ring in-plane bending, the combination of NH_2 twisting, and H−N^4−C twisting, respectively. Two peaks near 658 and 684 cm^{-1} are relative to the N^4−H wagging and ring in-plane bending modes. The bands involving the S═C−S symmetric stretching, ring C^2−S stretching and S−C−S stretching modes are observed as weak bands at 430, 630, and 776 cm^{-1}, respectively. A strong peak at 1353 cm^{-1} contributes from ring in-plane bending, N(H_2)−C^2 stretching and N−H rocking modes. And the peak at 1391 cm^{-1} is assigned to the

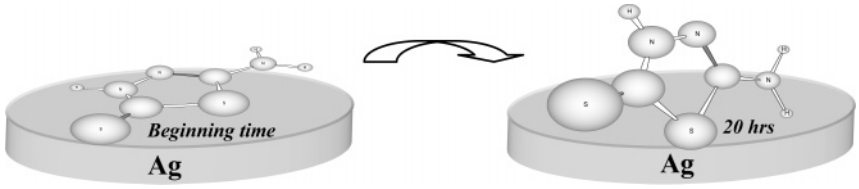

Figure 4. A proposed procedure for AMT molecule self-assembled on the silver surface with the going time.

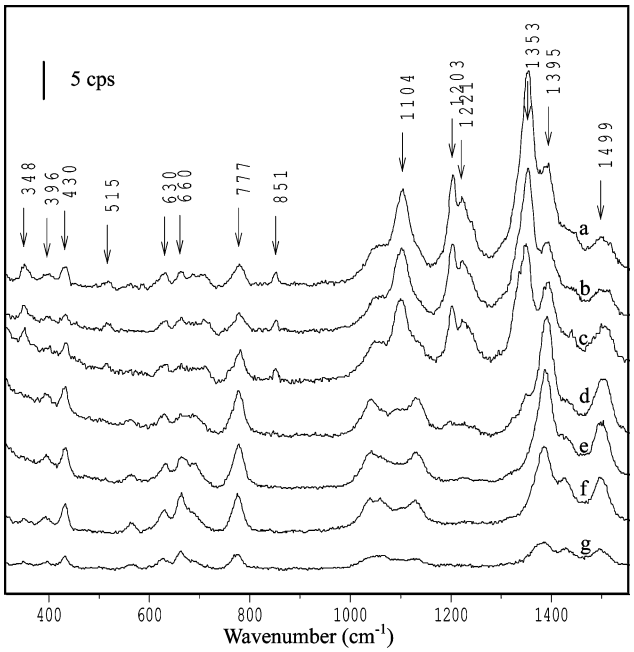

Figure 5. In situ SERS spectra of AMT absorbed at the Ag electrode surface in 0.1 mol L^{-1} KCl aqueous solution (a) open circuit potential (b) −0.1, (c) −0.2, (d) −0.3, (e) −0.4, (f) −0.5, and (g) −0.6 V vs SCE.

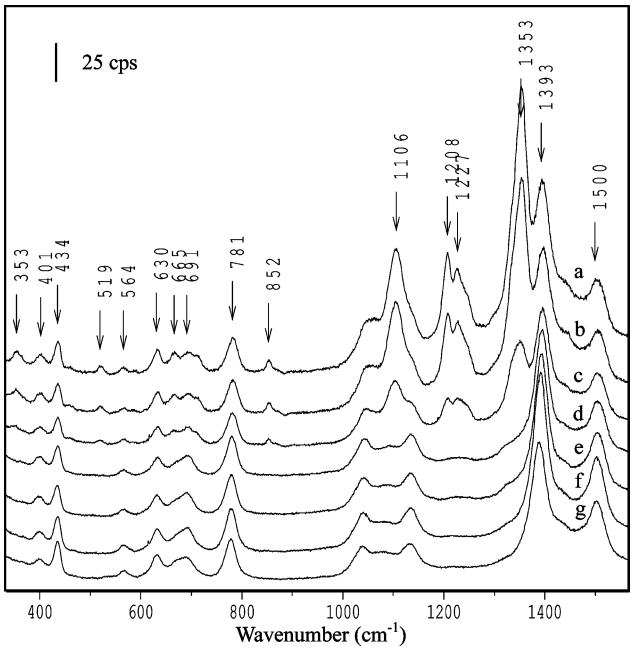

Figure 6. In situ SERS spectra of AMT absorbed at the Ag electrode surface in 0.1 mol L^{-1} KBr aqueous solution (a) open circuit potential (b) −0.1, (c) −0.2, (d) −0.3, (e) −0.4, (f) −0.5, and (g) −0.6 V vs SCE.

ring C^5-N^4 stretching mode. A shoulder band at 1043 cm^{-1} is attributed to S−C−S antisymmetric stretching mode. It should be mentioned that at 851 cm^{-1}, a weak peak is observed which is assigned to S−H rocking and NH_2 rocking in calculated

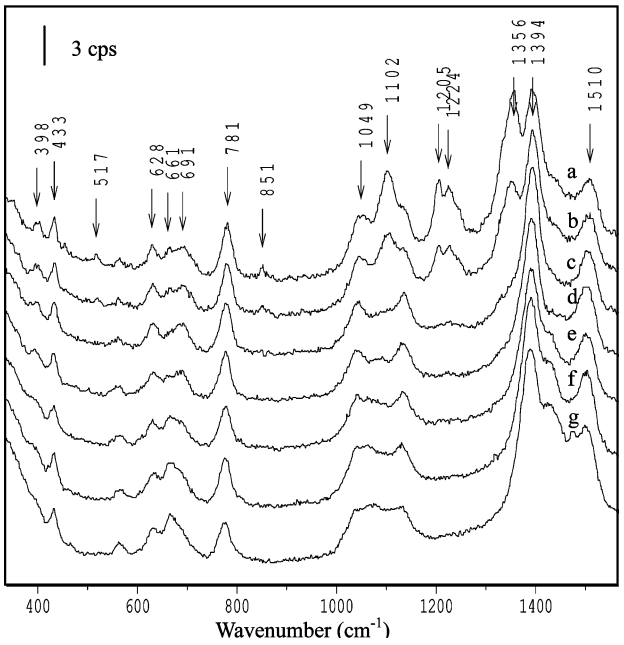

Figure 7. In situ SERS spectra of AMT absorbed at the Ag electrode surface in 0.1 mol L^{-1} $NaClO_4$ aqueous solution (a) open circuit potential (b) −0.1, (c) −0.2, (d) −0.3, (e) −0.4, (f) −0.5, and (g) −0.6 V vs SCE.

results, herein should be from the interaction of the NH_2 group and the surface after cleavage of S−H. Due to no corresponding bands found in the calculated results of AMT by BLYP/6-311G method, however, a strong band at 1102 and double peaks around 1201 and 1223 cm^{-1} are approximately attributed to the NH_2 rocking mode and the N^3-C^4 stretching together with the N−H rocking, respectively, based on the PM3 calculation for AMT vibrations. It is widely recognized that chemical moieties or groups closely access or directly adsorb on the electrode surface will be greatly enhanced.[36] Therefore, the assignments above of the peaks in the spectra suggest that after 20 h, the AMT molecules should finally anchor the Ag surface via the two sulfur atoms and a nitrogen atom in the amino as a tilted orientation with respect to the surface, since the appearance of the enhancement peaks seen in the in-plane and out-of-plane modes. A schematic way for the adsorption varying with the self-assembling time is illustrated in Figure 4. The change above could be regarded as the consequence of re-organization due to the increasing density and compact of AMT monolayers with the self-assembling processing.

In Situ Potential-Dependent SERS of AMT. For better understanding, the stability of AMT monolayers on the silver surface and the potential depentent SERS spectra, shown in Figure 5, were investigated in 0.1 mol L^{-1} KCl solution. At open circuit potential, the spectrum identified with Figure 3i, marks that the AMT molecules adsorbed onto the Ag surface through the two sulfur atoms and a nitrogen atom in the amino with a tilted orientation.

In the applied potential from −0.1 to −0.2 V, the intensities of the bands are decreasing in the high-frequency region, but

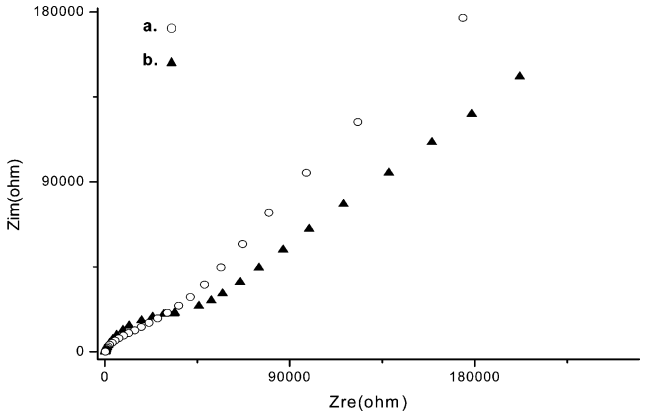

Figure 8. Nyquist impedance plots of Ag electrode: (a) blank and (b) with AMT monolayers in 0.1 mol L^{-1} KBr solution.

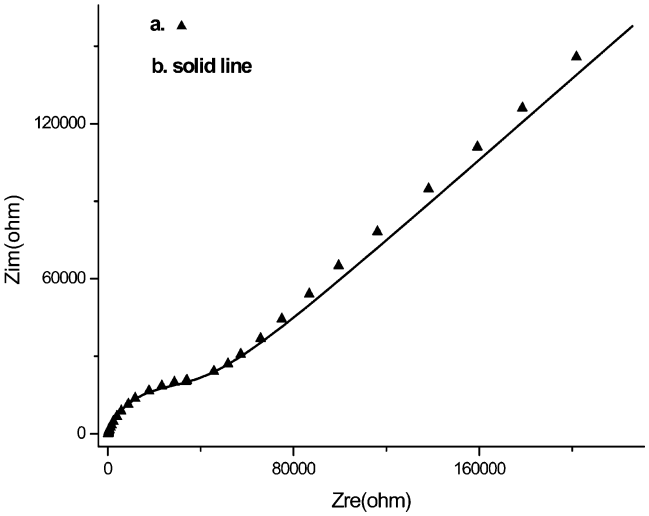

Figure 9. Nyquist impedance plots of AMT monolayers on the Ag electrode in 0.1 mol L^{-1} KBr solution: (a) experimental data and (b) curve fitting results.

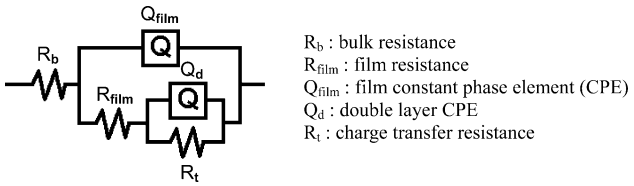

Figure 10. Equivalent circuit for curve fitting.

little change happens in the low frequency. The strong peak at 1353 cm^{-1} due to the ring in-plane bending combining with N−C[2] stretching and N−H rocking, weakens sharply and then disappears completely at −0.3 V. The complete disappearances of those bands at 1104, 1203, and 1221 cm^{-1} all due to N−H rocking mode and also the weak bands at 348 and 515 cm^{-1} assigned to N−H wagging, ring out-of-plane bending, NH_2 and H−N[4]−C twisting modes, are all invisible in Figure 5e. It is noticeable that with the absence of peak at 1104 cm^{-1}, a novel broad peak is observed at 1131 cm^{-1}, attributed to co-contribution of the NH_2 rocking and C═N−N antisymmetric stretching modes. The intensity of the NH_2 bands in high-frequency region decreases dramatically together with the occurrences of SERS bands relative to ring bending upon negative going potentials. The aforementioned phenomenon should attribute to the result of AMT ring toward the surface closer as well as the tendency of the NH_2 group away from the surface slightly due to the potential modulation resulting in the reorientation of the molecules. Little change for vibrations of the sulfur atoms on the ring and the thiol group in the low-frequency implies that the sulfur atoms still adsorb on the surface. Generally speaking, after the potential reaches −0.3 V, the orientation of ring first changes to an almost horizontal position, and the nitrogen atom is apart from the silver surface; however, the molecule remains anchoring at the silver surface through the two sulfur atoms. This proposal is in agreement with the well-known stability of thiolates on the surface of group IB metals.[37] With the potential held more negatively, the bands become even weaker. Until the applied potential reaches −1.1 V, the vibrational modes of AMT completely quenched in the SERS spectrum, meaning that the interaction between the AMT molecules and the silver vanished and AMT assembled monolayer has desorbed.

To explore the influence of the anions, in situ SERS experiments were performed in other electrolyte such as KBr solution herein and displayed in Figure 6. It is unambiguously found that both in KCl and in KBr solutions, the SERS spectral features and desorption steps with potentials are very similar by reason of bromine being in the same group of chlorine.

Perchlorate anion has been reported to coadsorb with imidazole by forming intermolecular hydrogen bonding.[17] In the interest of further investigating the possible co-adsorption of AMT with perchlorate anion, the potential-dependent in situ SERS spectra in ClO_4^- aqueous solution were carried out and shown in Figure 7. After adding ClO_4^- solution on the silver surface at open circuit potential, the enhanced peak at 1356 cm^{-1} weakens sharply comparing with the case in the KCl or KBr solutions, which may result from interaction of ClO_4^- and relatively positive charged NH_2 group of AMT under the medium about pH 4 in this experiment. Only at potential applied at −0.2 V, because of the change of adsorption mode of the molecule, do the bands representing the amino group in Figure 7 diminish, which is quite simliar to the case of the desorption process of AMT monolayers on Ag surface in the KCl or KBr solutions but the potential value at −0.3 V (vide ante). However, there is no co-adsorption of the ClO_4^- anions, and the AMT molecules existing because no ClO_4^- band around 933 cm^{-1} visualizes in all spectra.

Electrochemical Impedance Spectroscopy. The anticorrosive effect of AMT film was studied by electrochemical impedance spectroscopy. Figure 8 shows EIS plots in Nyquist format recorded on the modified silver/blank electrode in 0.1 mol L^{-1} KBr solution as well as in 0.1 mol L^{-1}KCl and $NaClO_4$ solutions (not given here due to similarity). The plot

TABLE 2: Values of Electrochemical Parameters for AMT Monolayers on the Ag Surface Obtained by Fitting the Experimental Impedance Data Using the Suggested Equivalent Circuit[a]

		Q_{film}			Q_d		
solution KBr	R_b (Ω cm^2)	Y_{film}[b]	n	R_{film} (Ω cm^2)	Y_d[b]	n	R_t (Ω cm^2)
0.1 mol L^{-1}	215.4	8.889×10^{-7}	0.81	$3.191\ 10^4$	1.562×10^{-5}	0.43	4.189×10^{11}

[a] Subscript b, effects of bulk solution; film, effects of film; d, effects of double layer; t, effects of charge transfer. [b] The dimensions are $S\ s^n$ (cm^2); if $n = 1$, they are F (cm^2).

of blank silver surface is approximate a beeline, with only a very small semicircle at high-frequency region. In contrast, in the impedance plot of AMT monolayers at the electrode, a more distinct Nyquist semicircle is shaped at higher frequency in the solution, demonstrating that the presence of inhibitor greatly changed the corrosion kinetics on the electrode surface.

The EIS data recorded in 0.1 mol L^{-1} KBr solution was analyzed by the software ZsimpWin and the curve fitting results is shown in Figure 9. The clear semicircle at high-frequency range should be due to the inhibitor film, because a dielectric film usually has a small time constant and then has a phase angle shift in this region. The impedance characteristic of this electrode surface was modeled by the equivalent circuit as shown in Figure 10. By comparing the circuit with the similar work,[38] film capacitance (C_{film}) and double layer capacitance (C_d) have changed to Q_{film} and Q_d [Q(CPE, con)], indicating that there is a barrier which the electrons impossibly drill through onto the electrode surface. The fitting results of impedance parameters were tabulated in Table 2.

4. Conclusion

In present work, the SERS technique was employed to elucidate the adsorption behavior of AMT at the silver surface. The self-assembling process was monitored by in situ SERS measurement. The stability and anticorrosive mechanism of the AMT monolayers on the silver surface were studied using the potential-dependent SERS and EIS spectroscopies, respectively. Some conclusions could be drawn as follows:

1. After about 20 h of self-assembling, the final structure of AMT monlayers formed at the silver surface in tilted mode through both sulfur atoms of thiol and thiadiazole ring, together with the nitrogen atom of amino.
2. In situ SERS spectra indicate that the orientation of the adsorbed AMT molecules experienced from a tilted adsorption way to a more horizontal fashion for thiadiazole ring with the NH_2 group of the AMT molecules slightly away from the surface, while the potential is shifted to the due voltage around -0.2 or -0.3 V vs SCE in different electrolyte solutions.
3. Electrochemical impedance spectroscopy for evaluating anticorrosion shows a promising inhibition effect whose mechanism is in agreement with theoretic fitting of R(Q(R(QR))) by ZsimpWin software.

Acknowledgment. This work was supported by Natural Science Foundation in Shanghai (Grant No. 06JC14094), the Foundation of Shanghai Higher Education (Grant No. 06ZZ18), and Shanghai Leading Academic Discipline Project (Grant No. T0402).

References and Notes

(1) Ganorkar, M. C.; Pandit, R. V.; Gayathri, P.; Sreenivasa, R. T. A. *Stud. Conserv.* **1988**, *33*, 97.
(2) Bastidas, J. M.; Otero, E. *Mater. Corros.* **1996**, *47*, 333.
(3) Otero, E.; Bastidas, J. M. *Mater. Corros.* **1996**, *47*, 133.
(4) Pandit Rao, V.; Sreenirasa Rao, T. A.; Ganorkar, M, C. *Trans. SAEST* **1992**, *7*, 222.
(5) Gajendragad, M. R.; Agarwala, V. *Indian J. Chem.* **1975**, *13*, 1331.
(6) Gajendragad, M. R.; Agarwala, V. B. *Chem. Soc. Jpn.* **1975**, *48*, 1024.
(7) Downie, T. C.; Harrison, W. *Acta. Crystallogr, Sect. B* **1972**, *28*, 1584.
(8) Edwards, H. G. M.; Jahanson, A. F.; Lawson, E. E. *Mol. Struct.* **199**5, *351*, 51.
(9) Prado, A. G. S.; Sales, J. A. A.; Carvalho, R. M.; Rubim, J. C.; Airoldi, C. J. *Non-Cryst. Solids* **2004**, *333*, 61.
(10) Thomas, S.; Biswas, N.; Venkateswaran, S.; Kapoor, S.; Naumov, S.; Mukherjee, T. J. *Phys. Chem. A* **2005**, *109*, 9928.
(11) Chowdhury, J.; Sarkar, J; De, R.; Ghosh, M.; Talapatra, G. B. *Chem. Phys.* **2006**, *330*, 172.
(12) Kudelski, A. *Langmuir*. **2003**, *19*, 3805.
(13) Baia, M.; Baia, L.; Kiefer, W.; Popp, J. *J. Phys. Chem. B* **2004**, *108*, 17491.
(14) Seballos, L.; Olson, T.; Zhang, J. Z. *J. Chem. Phys.* **2006**, *125*, 234706.
(15) Pergolese, B.; Miranda, M. M.; Bigotto, A. *J. Phys. Chem. B* **2006**, *110*, 9241.
(16) Kim, K.; Lee, H. S. *J. Phys. Chem. B* **2005**, *109*, 18929.
(17) Cao, P. G.; Gu, R. A.; Tian, Z. Q. *J. Phys. Chem. B* **2003**, *107*, 769.
(18) Fleischmann, M.; Hendra, P. J.; Mcquillan, A. *J. Chem. Phys. Lett.* **1974**, *26*, 163.
(19) Fleischmann, M.; Hill, I. R.; Mengoli, G.; Musiani, M. M.; Ahavan, J. *Electrochim. Acta.* **1985**, *30*, 879.
(20) Tian, Z. Q.; Ren, B.; Wu, D. Y. *J. Phys. Chem. B* **2002**, *106*, 9463.
(21) Jeanmaire, D. L.; Van Duyne, R. P. *J. Electroanal. Chem.* **1977**, *84*, 1.
(22) Nie, S.; Emory, S. R. *Science* **1997**, *275*, 1102.
(23) Kneipp, K.; Wang, Y.; Kneipp, H.; Perelman, L. T.; Itzkan, I.; Dasari, R. R.; Feld, M. S. *Phys. Rev. Lett.* **1997**, *78*, 1667.
(24) Ulman, A. *Chem. Rev.* **1996**, *96*, 1533.
(25) Ulman, A. *Acc. Chem. Res.* **2001**, *34*, 855.
(26) Sowerby, S. J.; Michael, E. W.; Wolfgang, M. H. *J. Phys. Chem. B* **1998**, *102*, 5914.
(27) Sung, M. M.; Sung, K.; Kim, C. G.; Lee, S. S.; Kim, Y. *J. Phys. Chem. B* **2000**, *104*, 2273.
(28) Saito, N.; Wu, Y.; Hayashi, K.; Sugimura, H.; Takai, O. *J. Phys. Chem. B* **2003**, *107*, 664.
(29) Diao, P.; Guo, M.; Tong, R. *J. Electroanal. Chem.* **2001**, *495*, 98.
(30) Cui, X. L.; Jiang, D. L.; Diao, P.; Li, J. X.; Tong, R. T.; Wang, X. K. *J. Electroanal. Chem.* **1999**, *470*, 9.
(31) Janek, R. P.; Fawcett, W. R. *J. Phys. Chem. B* **1997**, *101*, 8550.
(32) Boubour, E.; Lennox, R. B. *J. Phys. Chem. B* **2000**, *104*, 9004.
(33) Taniguchi, I.; Umekita, K.; Yasukouchi, K. *J. Electroanal. Chem.* **1986**, *202*, 315.
(34) Creighton, J. A. *Surf. Sci.* **1983**, *124*, 209.
(35) Moskovits, M.; Suh, J. S. *J. Phys. Chem.* **1984**, *88*, 5526.
(36) Yang, H. F.; Feng, J.; Liu, Y. L.; Yang, Y.; Zhang, Z. R.; Shen, G. L.; Yu, R. Q. *J. Phys. Chem. B* **2004**, *108*, 17412.
(37) Woods, R.; Hope, G. A.; Watling, K. J. *Appl. Electrochem.* **2000**, *30*, 1209.
(38) Wan, X. S.; Zhu, Y. F.; Shi, B. B.; Wan, L.; Xu, F. *Protein Mater. (in Chinese)* **2000**, *33*, 37.